Whale Optimization Algorithm for Maximum Power Point Tracker for Controlling Induction Motor Driven by Photovoltaic System

OSAMA EL-BAKSAWI

Electrical Engineering Department
Faculty of Engineering, Port-said University, Egypt.
osama.elbaksawi@gmail.com.

Abstract: This paper presents a new metaheuristics optimization algorithm for designing the maximum power point trackers, MPPT, with the photovoltaic system to feed an induction motor. This method is the whale optimization algorithm (WOA) which is motivated from the social behavior of the whales. The speed of induction motor is controlled by space vector pulse width modulation (SVPWM) with three level inverters. A sudden disturbance in mechanical torque of IM is done and the performance of MPPT in extracting the maximum power from the PV system is studied. The main reason of selecting the WOA is its simplicity in simulation. A comparative study is performed in case of replacing the PV system with a DC voltage source fed to the inverter. The obtained results ensure that the designed MPPT via the WOA is more efficient than DC voltage in feeding the 3-level inverter which is controlled by the SVPWM.

Keywords: Photovoltaic system; the whale optimization algorithm; space vector pulse width modulation.

1. INTRODUCTION

The photovoltaic systems gained a great attention in the last decades due to their clean generated power. In many applications, the photovoltaic (PV) system is connected to a motor for water pumping systems [1]. An induction motor driven by a PV system via an inverter is the most popular configuration for a water pumping system. In the last decades, pulse width modulation variable speed drives are taken place in many industrial applications. In the framework of the development in power electronic devices, circuits named multi-level inverters have become popular in many applications. Most of works deal with such systems as in the next paragraph. A PV water pump system [2] is presented in for village agricultural; the system comprises PV array, boost converter, three-phase inverter and induction motor based drive system. SVPWM is used to reduce the total harmonic distortion in the output signals of inverter; a constant voltage method has been used in simulating the maximum power point tracker (MPPT). In [3] the induction motor speed has been controlled via a presented Fuzzy Logic controller. A scalar control technique (V/F) is given in [4] to control the speed of 3-phase induction motor based on a voltage source inverter. A direct torque control of induction motor (IM) is simulated and presented in [5] for electric vehicles. Indirect vector control method with three-level cascade inverter has been used in [6] to control the induction motor speed, SVPWM method is used to control the inverter. A solar system fed an induction motor driven water pump system for nanofilteration system is presented in [7]; SVPWM is used to control the operation of both DC-DC converter and DC-AC inverter; additionally V/F control method is employed and MPPT based on Perturb and Observe (P&O) algorithm is presented. In [8] a PV system with MPPT based on P&O algorithm has been presented to supply an induction motor which is controlled via a state feed-back control strategy; Proportional Integral (PI) controller is incorporated in the system and its effect on the motor responses is studied. A Fuzzy Logic MPPT is designed in [9] to control the speed of the synchronous motor driven water pump system. In [10] a spice model of PV system with modified multilevel inverter and energy storage system has been built.

A maximum power point tracker, MPPT, based on the Whale Optimization Algorithm (WOA) is presented to track the maximum power extracted from the PV system. The PV system is connected to an induction motor via 3-level inverter. The inverter is controlled by SVPWM to obtain a constant speed of IM. A sudden disturbance in mechanical torque of motor is done and the performance of MPPT is studied. The PV system is replaced by a DC voltage source and the results are compared to those with PV system. The obtained results ensure that the designed MPPT via the WOA is more efficient than the DC voltage in feeding the 3-level inverter which is controlled by the SVPWM [11, 12].

2. MATHEMATICAL MODEL

In this section, the models of PV array and space vector pulse width modulation (SVPWM) are presented.

2.1 PV Array Model

It is assumed that a PV array of N_s series modules and N_p parallel branches, the two-diode model represented in [13] is used and the output current obtained from the PV array is given in the following formula:

$$I^A = N_p I_{ph} - N_p I_{o1}\left\{exp\left(\frac{V_A+I_A R_s{}^A}{\alpha_1 N_s V_{T1}}\right)-1\right\} - N_p I_{o2}\left\{exp\left(\frac{V_A+I_A R_s{}^A}{\alpha_2 N_s V_{T2}}\right)-1\right\} - \left\{\frac{V_A+I_A R_s{}^A}{R_p{}^A}\right\} \quad (1)$$

I_{ph} is the photon current, I_{o1}, I_{o2} are the saturation currents of two diodes model respectively, V_A, I_A are the PV array voltage and current respectively, α_1, α_2 are the diodes ideality factors, and V_{T1}, V_{T2} are the thermal voltages of each diode, $R_s{}^A$ and $R_p{}^A$ are the series and parallel resistances of the PV array nd given by:

$$R_s{}^A = \frac{N_s}{N_p} R_s{}^m \quad And \quad R_p{}^A = \frac{N_s}{N_p} R_p{}^m \quad (2)$$

Where $R_s{}^m$ and $R_p{}^m$ are the series and parallel resistances of the PV module respectively

2.2 Space Vector Pulse Width Modulation Model

2.2.1. Level diode clamped inverter

The 2-level voltage source inverter has been very popular in drives for many years due to its ease of implementation and control. However, 2-level inverters can be limited by the voltage ratings of the semiconductor devices, particularly in high power applications [14]. Multilevel inverters were developed to help addressing this concern as well as other limitations of 2-level inverters. In particular, 3-level inverters have been popular due to their improvement in output waveforms without overly complicating the design and control of the inverter [15].

The basic function of the 3-level inverter is very similar to the 2-level inverter. While the 2-level inverter switches the output phases between the positive dc bus and the negative dc bus, the 3-level inverter switches the output phases between the positive dc bus, the negative dc bus, and the neutral point of the bus. The basic strategy of three-level space vector PWM is identical to that of two-level space vector PWM. A rotating reference vector formed from three sinusoidal sources is approximated over sampling period *Ts* using linear combinations of voltage vectors [16]. The reference vector is written as follows:

$$V_{ref} = V_{ref}\, e^{j(\omega_e t+\phi)} \quad (3)$$

To simplify the three-level space vector PWM logic, the three-level hexagon of voltage vectors is divided into six smaller hexagons. Three of these smaller hexagons are shown in Fig. 1. Each of these smaller hexagons is centered at the tips of the small vectors and consists of six equilateral triangles corresponding to the six sectors of a two-level inverter.

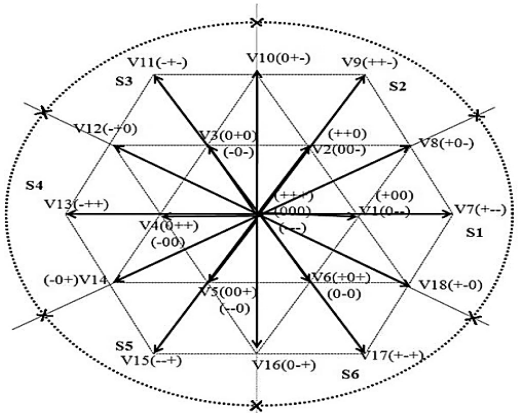

Fig. 1 The three-level voltage vectors plotted in the (α−β) plane.

2.2.2. Switching table

The three phase 3-level diode clamped multilevel inverter is the common multilevel inverter used for various applications [17]. A three phase 3-level diode clamped multilevel inverter is adopted in this paper.

There are twelve active combinations were taken using these switching states which produce twelve active voltage vectors. The nonzero voltage vectors are from V_1 to V_{12}.

The switching Table is formed using the sector, the corresponding voltage vector and the switch state. For example, the angle of the reference voltage is between 0^o and 30^o, it is in sector 1 and it selects the voltage vector V_1. The corresponding switching state is 110000. Switches S_{a1} and S_{a2} are in on state. Switches S_{b1}, S_{b2}, $S_{c1}$and S_{c2} are in off state. Switches S_{a1}', S_{a2}', S_{b1}', S_{b2}', S_{c1}'and S_{c2}' are complementary [18]. The summary of various states are given in Table 1.

Table 1 3-Level Diode Clamped Inverter Switching Table

Sector	Voltage vector	Switche state					
		S_{a1}	S_{a2}	S_{b1}	S_{b2}	S_{c1}	S_{c2}
1	V_1	1	1	0	0	0	0
2	V_2	1	1	0	1	0	0
3	V_3	1	1	1	1	0	0
4	V_4	0	1	1	1	0	0
5	V_5	0	0	1	1	0	0
6	V_6	0	0	1	1	0	1
7	V_7	0	0	1	1	1	1
8	V_8	0	0	0	1	1	1
9	V_9	0	0	0	0	1	1
10	V_{10}	0	1	0	0	1	1
11	V_{11}	1	1	0	0	1	1
12	V_{12}	1	1	0	0	0	1
Note: $S_{a1}'=1-S_{a1}$, $S_{a2}'=1-S_{a2}$, $S_{b1}'=1-S_{b1}$, $S_{b2}'=1-S_{b2}$, $S_{c1}'=1-S_{c1}$, $S_{c2}'=1-S_{c2}$							

3. WHALE OPTIMIZATION ALGORITHM

The whale optimization algorithm (WOA) is a recent metaheuristics algorithm represented by Mirjalili et al. [19]. WOA simulates the humpback whales' social behaviors as it is motivated from the strategy of hunting followed by the whales. The hunting process is called bubble-net feeding method; the preferred food of the humpback whales is small fishes close to the water surface. The catching prey process is performed through creating bubbles along a circle which is classified in to two categories; upward spiral and double-loops. In the first jockey, the humpback whale dives down about 12 m and then creates bubble in a spiral shape around the victim and swim up to the surface. In the second jockey, there are three different stages which are coral loop, lob tail, and capture loop [20]. The current position of the victim is determined via the humpback whales. This position is updated to obtain the best search agent; the updating process is performed using the Equation (4).

$$\vec{X}^{k+1} = \overrightarrow{X_p}^{k} - \vec{A}.\left|\vec{C}.\overrightarrow{X_p}^{k} - \vec{X}^{k}\right| \qquad (4)$$

Where $\overrightarrow{X_p}^{k}$ the prey position vector at iteration k, $\vec{X}^{k}$ the prey position at iteration k, $\vec{A}$ and $\vec{C}$ are coefficient vectors which are determined as follows:

$$\vec{A} = 2\vec{a}.r - \vec{a} \qquad (5), \qquad \vec{C} = 2.r \qquad (6)$$

Where $\vec{a}$ is linearly decreased from 2 to 0 and r is a random vector in [0, 1]. The attack on the prey process is carried out by the method of bubble-net strategy or called exploration phase; in the exploitation phase two approaches are followed by humpback whales which are: mechanism of shrinking encircling which is given in equation (4) and the spiral updating position. The shrinking encircling is achieved by reducing the value of $\vec{a}$ from 2 to 0 as shown before and then the range of $\vec{A}$ is also decreased. In the second approach, the distance between the whale's location and the prey location is calculated to update the whale's position in a spiral path to devour the prey. The updating process is performed by the following eqn.

$$\vec{X}^{k+1} = \overrightarrow{X_p}^{k} + \left|\overrightarrow{X_p}^{k} - \vec{X}^{k}\right|.e^{bl}.cos(2\pi l) \qquad (7)$$

Where b is a constant that clarifies the shape of logarithmic spiral, l is a random value between [-1, 1]. The selection between two approaches is based on a probability index, Prob, as in case of Prob is less than 0.5 the first approach is taken place else the second one is performed. The searching action on the prey is called exploration phase which is achieved by varying the vector $\vec{A}$. It is known that the humpback whales search the prey in random manner therefore the values of vector $\vec{A}$ are randomly selected greater than 1 or less than -1 to oblige the search agent to move out of a reference whale. The whale's position is updated randomly as in case of the absolute of element in $\vec{A}$ vector is greater than unity the position is updated based on the following equation:

$$\vec{X}^{k+1} = \overrightarrow{X_{rand}}^{k} - \vec{A}.\left|\vec{C}.\overrightarrow{X_p}^{k} - \vec{X}^{k}\right| \qquad (8)$$

The flowchart shows the main steps followed in the whale optimization algorithm is shown in Fig. 2.

4. THE PROPOSED METHODODLOGY

The design variable is duty cycle fed to the DC-DC converter while the objective function is the power extracted from the PV array. The objective function can be written as follows [16]:

$$P_A(d) = V_o(1-d) * \left(\sum_{i=1}^{n}\left(\left(I_{ph} - I_{o1}\left\{exp\left(\frac{V_A+I_AR_sarr}{\alpha_1 V_{T1}}\right) - 1\right\} - I_{o2}\left\{exp\left(\frac{V_A+I_AR_sarr}{\alpha_2 V_{T2}}\right) - 1\right\} - \left\{\frac{V_A+I_AR_sarr}{R_{parr}}\right\}\right)\right)\right) \qquad (9)$$

Where V_o is the output voltage from the PV array, d is the converter dusty cycle. The value of duty cycle must be in ringed [0, 1].

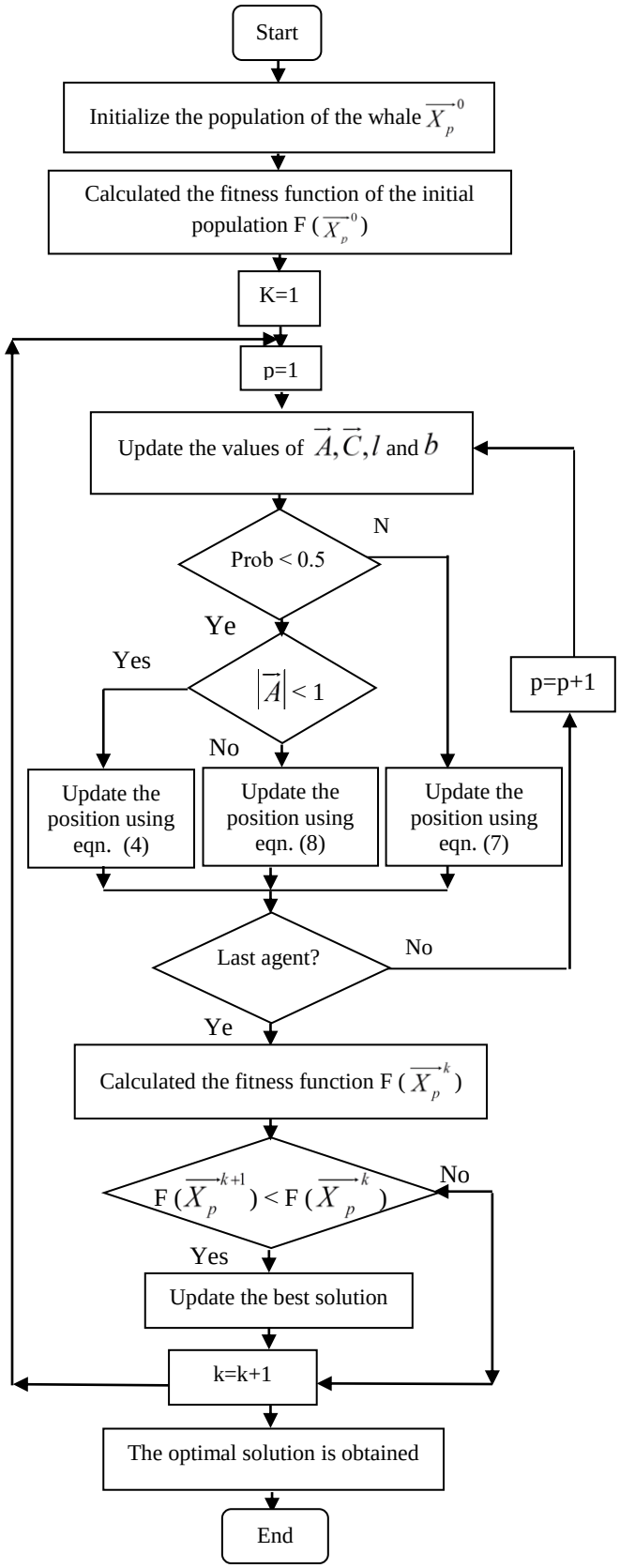

Fig. 2 The WOA flowchart

The block diagram of the proposed control strategy is given in Fig.3.

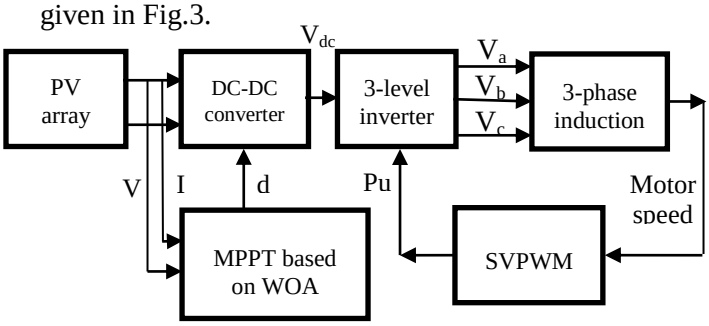

Fig. 3 The block diagram of the proposed control system

The PV array maximum power is obtained via the MPPT designed by the WOA by feeding the corresponding duty cycle to DC-DC converter after searching process. The converter output is the dc voltage at MPP fed to the inverter which controlled by the SVPWM based on the measured speed of the induction motor.

5. NUMERICAL ANALYSIS

The system under study comprises PV array with MPPT designed by WOA, DC-Dc converter, 3-level inverter and induction motor. The electrical specifications of system are given in Table 2 in appendix. The output voltage and current from the PV array are measured and fed to the WOA-MPPT based algorithm that search the duty cycle that gives the maximum power from the array. The duty cycle corresponding to maximum power is fed to the converter and the output DC voltage is fed to the inverter which is controlled via SVPWM control to obtain a constant speed of IM.

Table 2 Specifications of the system under test

Electrical specifications of PV array	
Module type	IM72C3-310- T12E
Ns	8
Np	4
Maximum power (W)	309.9630
Voltage at max. power (V)	37.3
Current at max. power (A)	8.31
Open circuit voltage (V)	45.22
Short circuit current (A)	8.9
R_s^m (Ω)	0.0092
R_p^m (Ω)	2562.3

DC-DC Converter parameters	
Input capacitor (μf)	100
Inductance (mh)	1
Output capacitor (μf)	2300
Induction motor parameters	
Rated power (W)	3730
Line voltage (V)	350
Frequency (Hz)	50
Stator resistance (Ω)	1.115
Stator inductance (h)	0.005974
Rotor resistance (Ω)	1.083
Rotor inductance (h)	0.005974

It is assumed that the IM electromagnetic torque is changed from 0 to 3 causes the changing the IM reference speed from 160 rpm to 150 rpm at t=1 sec. The DC voltage supplied at the inverter terminal is given in Fig. 4; it is shown that the voltage is fixed at time 0.6 sec. at 443 V after searching the required converter duty cycle and at t= 1 sec. the voltage becomes transient and then returns to its steady value of 429 V after 1.2 sec.

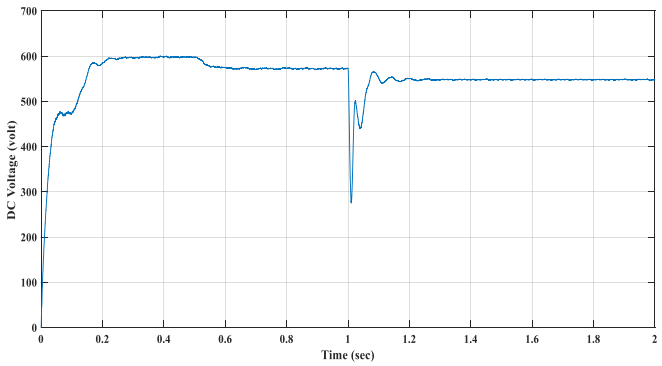

Fig. 4 DC output voltage from the converter

The stator currents of IM are shown in Fig. 5, the electromechanical torque of motor is shown in Fig. 6 while Fig. 7 shows the IM speed variation with time; referring to Fig. 7 it is cleared that the proposed SVPWM is succeeding in tracking the reference speed of the IM. In order to ensure the superiority of utilizing a PV system with maximum power point tracker based on the proposed methodology incorporated the WOA, the PV system is replaced by a constant DC voltage source of value 600 V input to the inverter and the same SVPWM control methodology is performed. The obtained results are compared to those obtained via the PV system.

The rotor speed of IM in the two cases is given in Fig. 8; it is shown that response of the speed with a designed PV system is better than that obtained in case of using a DC voltage source as it reaches to the steady state vales faster than the first one, additionally the transient response with using the PV system is less than that obtained in using the DC source.

This is due to the proposed WOA-MPPT based controller which gives the flexibility of changing the DC voltage fed to the inverter to adapt to the sudden disturbance in the IM speed. Additionally; the electromagnetic torques effect on the IM in two studied cases are shown in Fig. 9 which ensure the improved response via the PV with MPPT system.
The stator current of each phase in the two cases is shown in Fig. 10, it is noted that the transient response of the current in case 1, using DC voltage source, is larger than that obtained in case 2.

A comparative study of the obtained time responses' performance specifications including rise time, settling time, over shoot and under shoot with two studied cases is performed and tabulated in Table 3.

Referring to the obtained results one can get that; the obtained results via the using of the PV system is better than those of Dc source. Therefore; it is derived that the PV system with MPPT designed via the WOA is suitable for controlling the IM speed with the presented SVPWM than the usage of the constant DC voltage source.

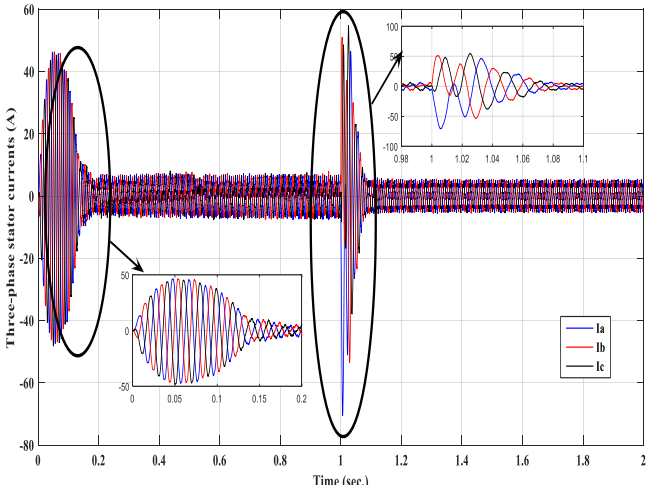

Fig. 5 The 3-phase stator current of IM

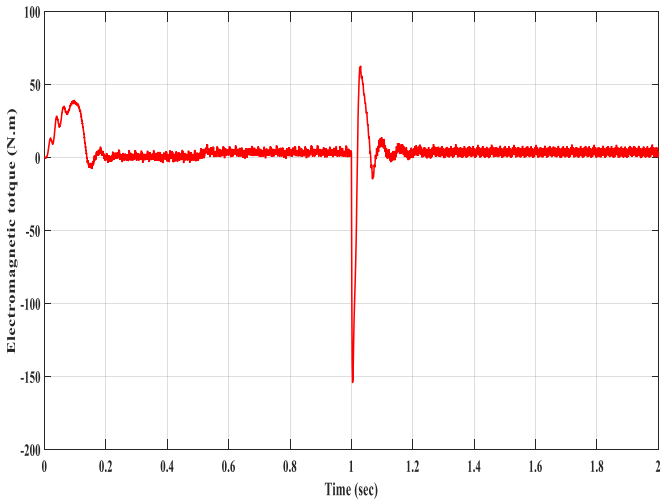

Fig. 6 The electromagnetic torque of the IM

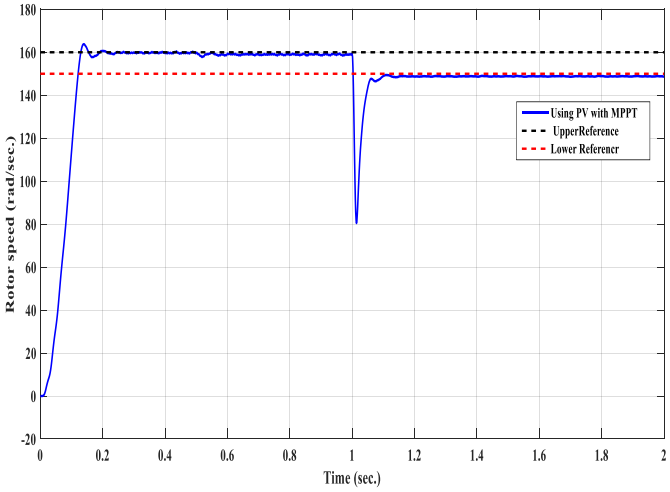

Fig. 7 The IM rotor speed

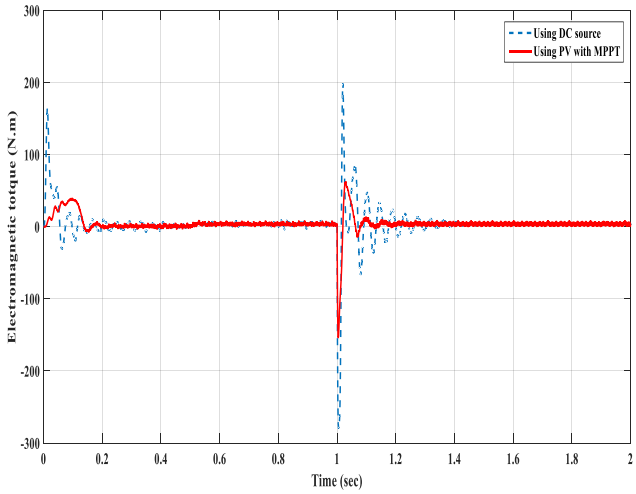

Fig. 8 The rotor speed in case of usage the DC source and with PV system

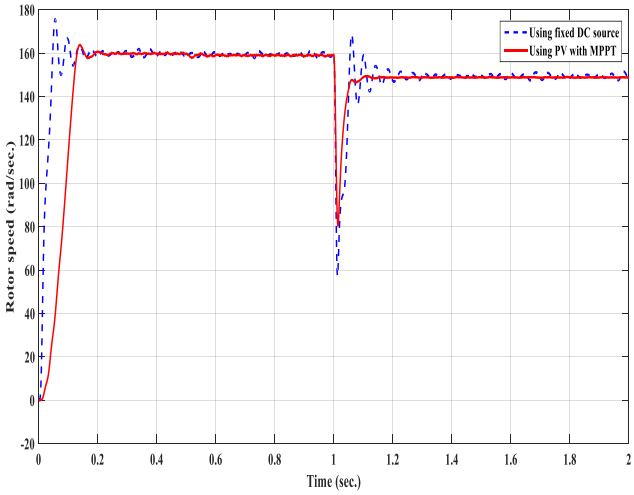

Fig. 9 The IM electromagnetic torque in case of usage the DC source and with PV system

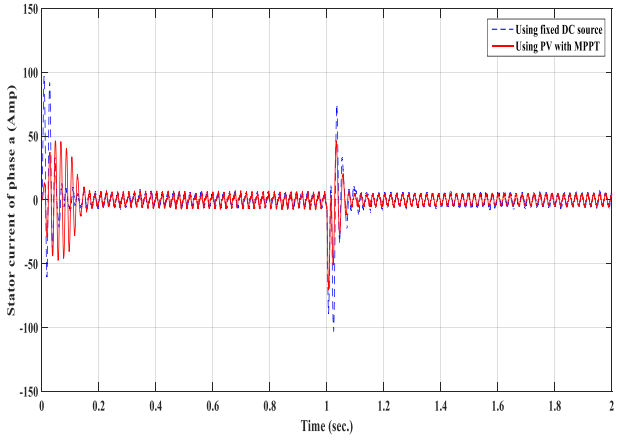

(a)

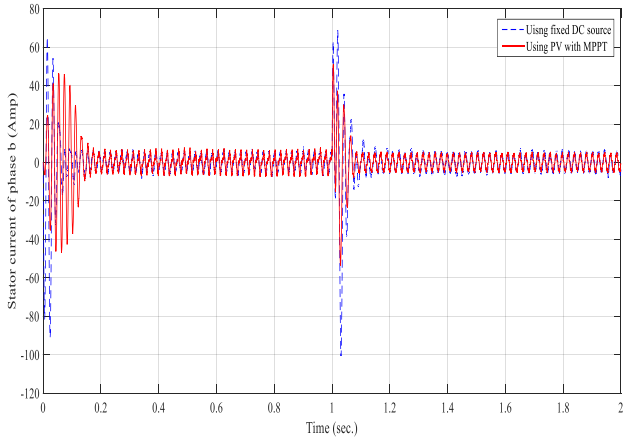

(b)

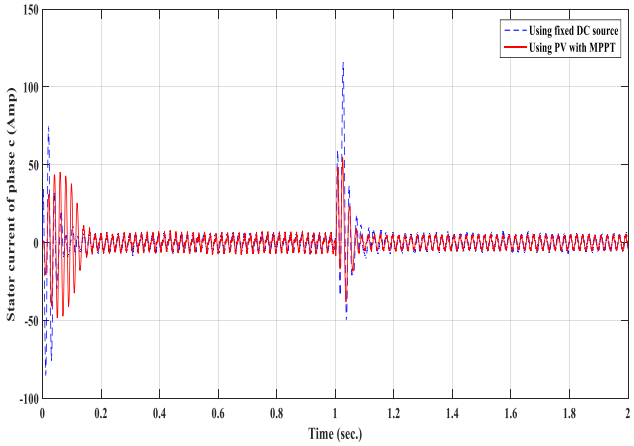

(c)

Fig. 10 IM stator current in case of usage the DC source and with PV system (a) phase no. 1 (b) phase no. 2 (c) phase no. 3

Table 3 A comparative study of the performance specification

Performance specifications of the rotor speed response		
	DC source	PV
	Before applied torque	
Overshoot (rad/sec.)	175	165
Undershoot (rad/sec.)	155	159
After applied torque		
Overshoot (rad/sec.)	165	150
Undershoot (rad/sec.)	60	80
Performance specifications of the electromagnetic torque		
	DC source	PV
	Before applied torque	
Overshoot (rad/sec.)	170	40
Undershoot (rad/sec.)	-25	10
After applied torque		
Overshoot (rad/sec.)	200	50
Undershoot (rad/sec.)	-280	-140
Performance specifications of the stator current		
	DC source	PV
	Before applied torque	
Overshoot (rad/sec.)	95	40
Undershoot (rad/sec.)	-60	-45
After applied torque		
Overshoot (rad/sec.)	75	50
Undershoot (rad/sec.)	-100	-70

6. CONCLUSION

This paper presents an optimization algorithm for simulating the maximum power point trackers with the photovoltaic system to feed an induction motor and comparative study between this control method and SVPWM based speed control of induction motor with 3-Level Inverter using DC source. Control methods have been simulated by using control system design based on MATLAB software.

Study is summarized as follows: -

1. By using the designed PV system is preferred over other controlling scheme for high dynamic applications.
2. Photovoltaic system with the whale optimization algorithm strategy reduced ripples for the torque by ten times when compared with SVPWM based speed control of induction motor with 2-Level Inverter using DC source.
3. In the speed curve has a lower ripple in the case of Photovoltaic system and reduced by three times when compared other controlling scheme and Photovoltaic system has a lower over shoot after applied torque.
4. Ripple of stator current in the case of Photovoltaic system reduced and over shoot has lower when compared other controlling scheme and reduced by four times.
5. As mention in Table 4 Photovoltaic system with the whale optimization algorithm strategy is best if compared with with SVPWM based speed control of induction motor with 2-Level Inverter using DC source.

7. REFERENCES

[1] W. Xiao, F. F. Edwin, G. Spagnuolo, J. Jatsvevich. Efficient approach for modelling and simulating photovoltaic power system. IEEE Journal of Photovoltaics, vol. 3, no. 1, pp. 500-508, Jan. 2013.

[2] G. M. Masters. “Renewable and efficient electric power systems”. John Wiley & Sons, Inc., Hoboken, New Jersey, 2004.

[3] D. V. Ram, B. V. Ramana. V/F speed control of SVPWM based solar fed induction Motor. International Journal of Application or Innovation in Engineering & Management, vol. 3, no. 11, 2014, pp. 236-242.

[4] R.Jayashree, S.Mumtaj. Implementation of digital PWM speed control strategy for survivable induction motor drives. International Journal of Advanced Research in Electrical, Electronics and Instrumentation Engineering, vol. 2, no. 11, 2013, pp. 5569-5576.

[5] S. K. Soni, A. Gupta. Analysis of SVPWM based speed control of induction motor drive with using V/F control based 3-level inverter. International Journal of Scientific Engineering and Technology, vol. 2, no.9, 2013, pp. 932-938.

[6] M. L. Swarupa, G. T. R. Das, P.V. R. Gopal. Simulation and analysis of SVPWM based 2-level and 3-level inverters for direct torque of induction motor. International Journal of Electronic Engineering Research, vol. 1, no. 3, 2009, pp. 169-184.

[7] C. S. Parimala, M. H. Reddy. Performance of induction motor using 3-level cascade inverter. International Journal of Engineering Research and Applications, vol. 3, no. 4, 2013, pp. 2069-2075.

[8] C. Jin, B. Wang, D. Jiang, W. Jiang. Energy conversion stage design of solar water pump in a nanofiltration system. Energy Procedia, vol. 12, 2011, pp. 1049–1056.

[9] A. Larabi, K. Yazid, M.S. Boucherit. Speed sensorless control with a linearization by state feedback of induction machine with adaptation of the rotor time constant using fuzzy regulator powered by photovoltaic solar energy. Energy Procedia, vol. 18, 2012, pp. 235–244.

[10] H. Bouzeria, C. Fetha, T. Bahi, I. Abadlia, Z. Layate, S. Lekhchine. Fuzzy logic space vector direct torque control of PMSM for photovoltaic water pumping system. Energy Procedia, vol. 74, 2015, pp. 760–771.

[11] D. Iero, R. Carbone, R. Carotenuto, C. Felini, M. Merenda, G. Pangallo, F. G. D. Corte. SPICE modelling of a complete photovoltaic system including modules, energy storage elements and a multilevel inverter. Solar Energy, vol. 107, 2014, pp. 338–350.

[12] M. Valan Rajkumar, P.S. Manoharan, A. Ravi. Simulation and an experimental investigation of

SVPWM technique on a multilevel voltage source inverter for photovoltaic systems. Electrical Power and Energy Systems, vol. 52, 2013, pp. 116–131.

[13] I. Colak, E. Kabalci, R Bayindir. Review of multilevel voltage source inverter topologies and control schemes. Energy Conversion and Management, vol. 52, 2011, pp. 1114–1128.

[14] A. Fathy, H. Rezk. A novel methodology for simulating maximum power point trackers using mine blast optimization and teaching learning based optimization algorithms for partially shaded photovoltaic system. Journal of Renewable and Sustainable Energy, vol. 8, no. 2, 2016, pp. 1-16.

[15] S. Elangovan, K. Thanushkodi, A Novel direct power control of 3 phase induction multi motor drive with AFF. International Journal of Soft Computing and Engineering, vol. 3, no.2, 2013, pp. 124–127.

[16] Adel Mehdi, Salah-eddine Rezgui, Houssam Medouce, and Hocine Benalla. A Comparative Study between DPC and DPC-SVM ControllersUsing dSPACE (DS1104). International Journal of Electrical and Computer Engineering, vol. 4, no. 3, 2014, pp. 322–328.

[17] R. Dharmaprakash, J. Henry. Switching table based 2-level inverter and 3-level diode clamped inverter. Journal of Theoretical and Applied Information Technology, vol. 60, no. 2, 2014, pp. 380–389.

[18] G.Goutham Kumar Reddy, S.Sridhar. Three Level Modified SVPWM Inverter Fed DTC Induction Motor Drive. International Research Journal of Engineering and Technology, vol. 02, no. 6, 2015, pp. 321–327.

[19] S. Mirjalili, A. Lewis. The Whale Optimization Algorithm. Advances in Engineering Software, vol. 95, 2016, pp. 51–67.

[20] J. A. Goldbogen, S. Friedlaender, J. Calambokidis, M. F. McKenna, M. Simon, D. P. Nowacek. Integrative approaches to the study of baleen whale diving behavior, feeding performance, and foraging ecology. Bioscience, vol. 63, no. 2, 2013, pp. 90-100.